SUPPLEMENTARY INFORMATION

Unraveling the folding-assisted unbinding mechanism of TCF with its binding partner β-catenin

Amal Vijay and Arnab Mukherjee*

arnab.mukherjee@iiserpune.ac.in

Department of Chemistry, Indian Institute of Science Education and Research, Pune-411008, India.

I. Representation of residues utilized for defining collective variables

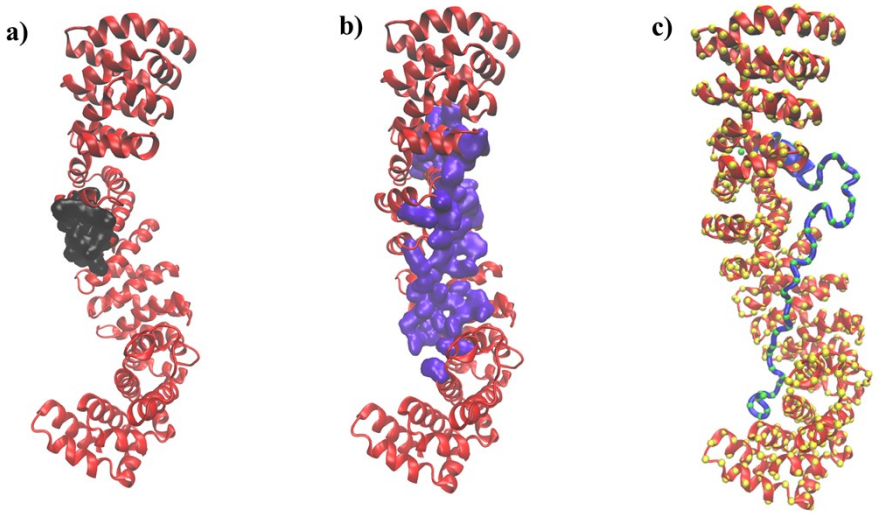

Fig. S1: Representation of residues involved in the construction of collective variables. β-catenin and TCF are shown in red and blue, respectively. a) Residue numbers 312, 313, 315, 316, 321, 347, 348, 350-358 in β-catenin (highlighted in black color for the construction of $\boldsymbol{X}$). b) Residue numbers 219, 253, 254, 256, 257, 260, 261, 264, 265, 290, 292, 293, 295, 296, 299, 302, 303, 306, 307, 312, 333, 335, 338, 339, 342, 345, 346, 349, 354, 376, 383, 386, 387, 389, 390, 393, 422, 425, 426, 428-430, 435, 462, 463, 466, 469, 470, 473, 474, 508, and 568 in β-catenin (highlighted in violet color, for the construction of $\boldsymbol{X}$). c) Cα atoms present in the β-catenin: TCF complex. Cα atoms present in the β-catenin and TCF are shown in yellow and green, respectively. Cα atoms were used for the construction of $\boldsymbol{N_c}$ and $\boldsymbol{R_g}$.

II. Clustering of states

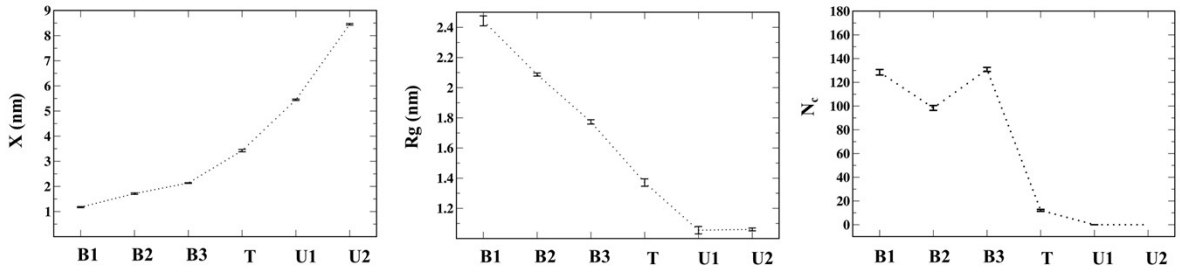

Figure S2. Ranges of biased collective variables (X, N_c, and R_g) values in the states B1, B2, B3, T, U1 and U2.

III. Convergence of free energy profiles

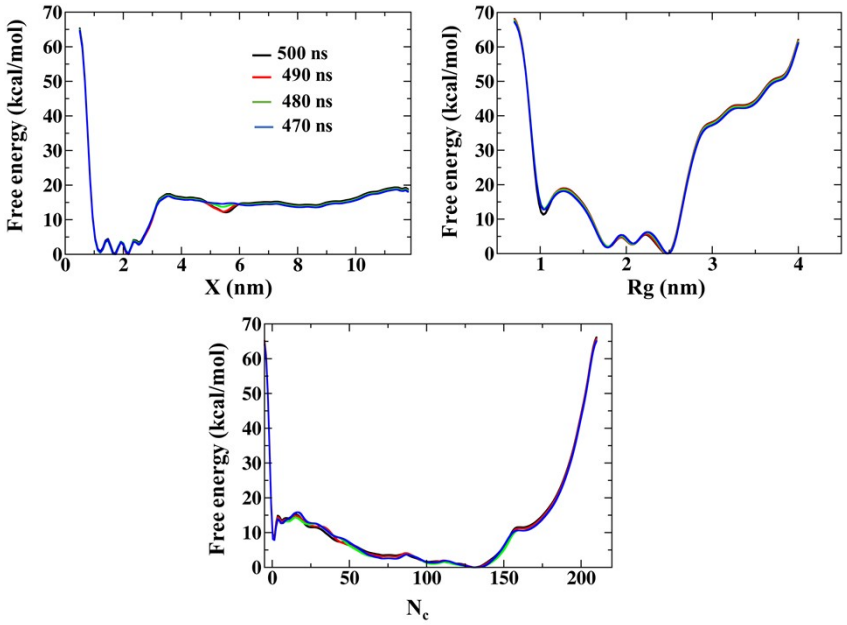

Figure S3. Free energy profiles at different time instances with respect to biased collective variables indicate the convergence of simulation.

IV. Variation of interaction energy during the unbinding pathway

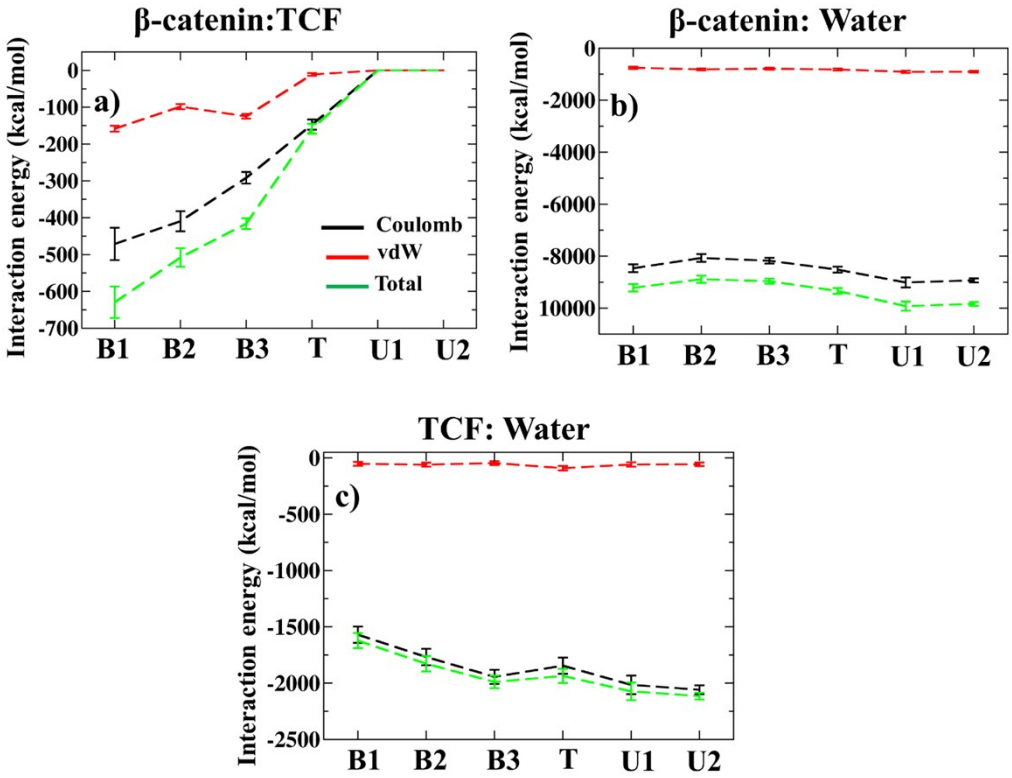

Figure S4. Variations of Coulomb, van der Waals (vdW), and total interaction energy profiles along the unbinding pathway for a) β-catenin and TCF, b) β-catenin and water, and c) TCF and water.

V. Intermolecular and intramolecular contacts between the residues in β-catenin:TCF complex during unbinding pathway

Heatmaps depicting the contacts between β-catenin (residues 140-663) and TCF (residues 1-49) during the unbinding pathway is shown in Figs S5 and S6, utilizing a 2 nm cut-off distance. Figure S5 reveals no significant change within the residues of β-catenin. However, the contacts between β-catenin and TCF are lost during the unbinding pathway (from B1 to U2). Subsequently, intramolecular contacts are established within TCF, aiding the folding process. Importantly , an increased number of intermolecular contacts are observed within residues 25 to 35 of TCF in states U1 and U2 (Fig. S6).

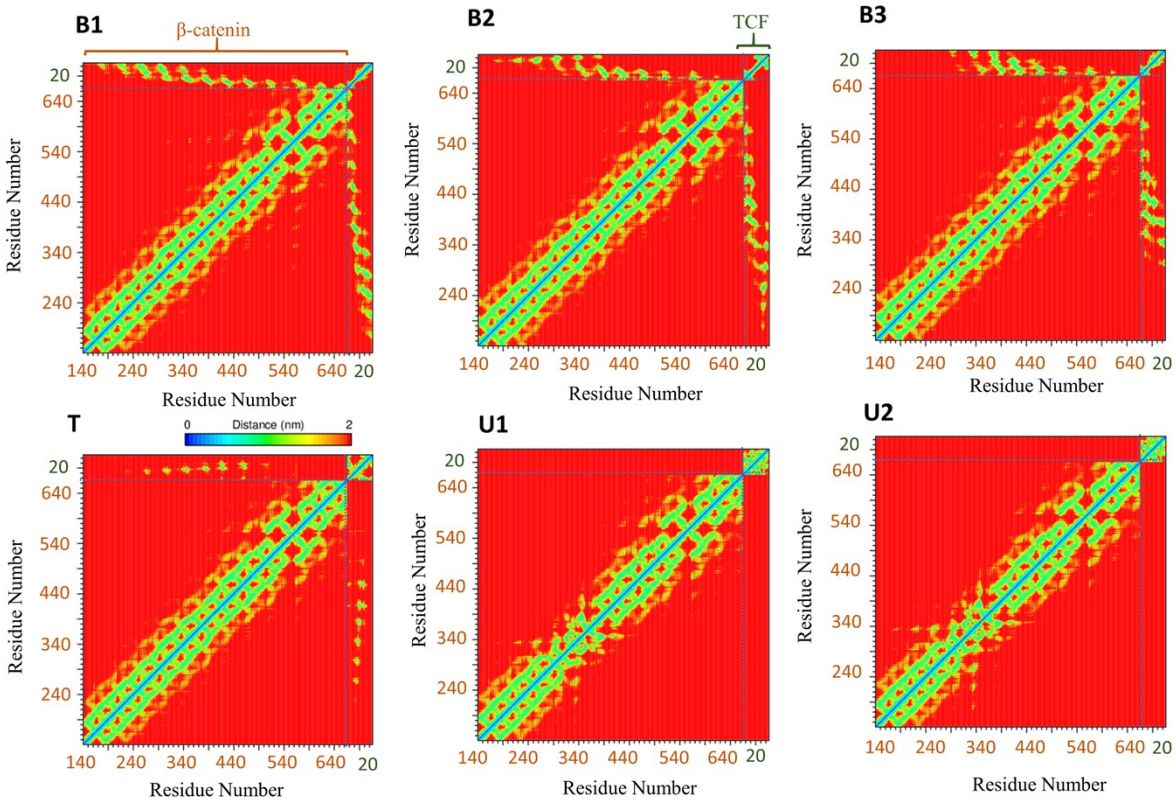

Figure S5. Contact map between the residues in the β-catenin:TCF complex during the unbinding pathway. Residue numbers 140 to 663 indicate the residues in β-catenin. Residue numbers 1 to 49 indicate the residues in TCF. Intermolecular contacts between β-catenin and TCF has been lost in the unbound states. β-catenin and TCF residues are marked above the contact maps of B1 and B2 states respectively.

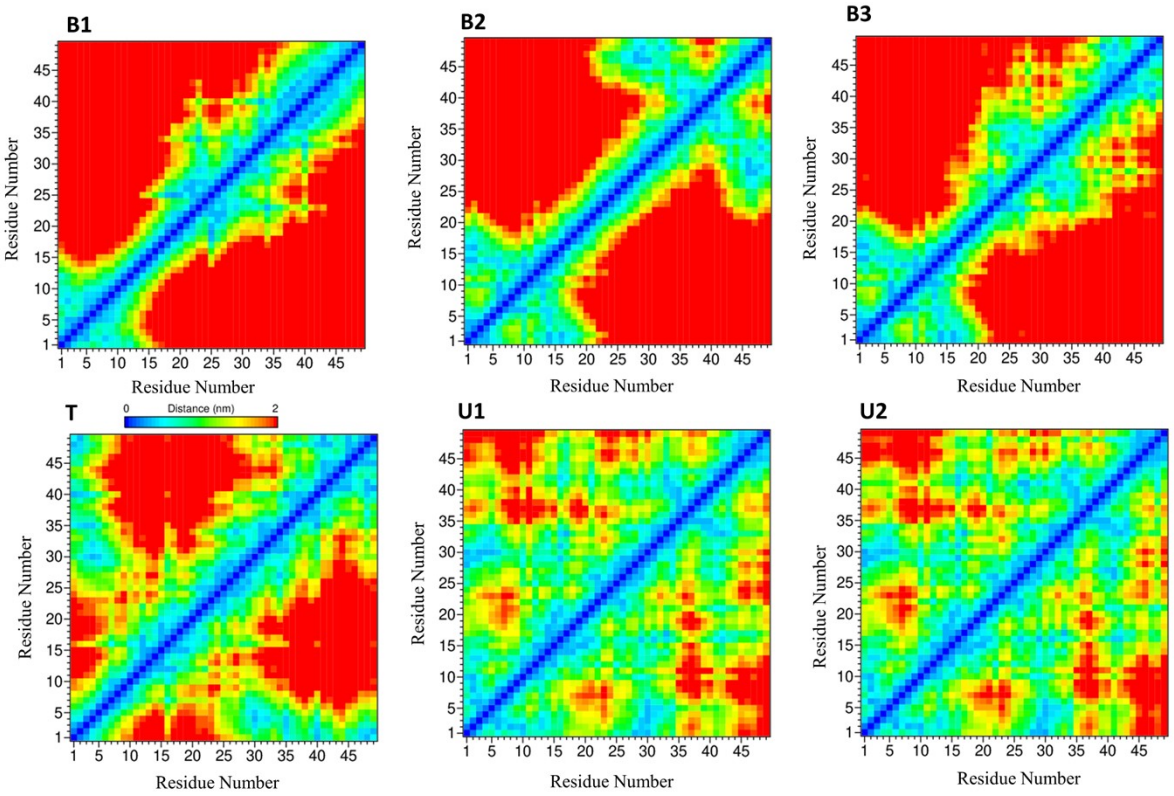

Figure S6. Intramolecular contact map between the residues of TCF (residue numbers 1 to 49) during the unbinding pathway. An increase in contacts is observed in the unbound states compared to bound state and transition state.

The percentage of specific residues of β-catenin that interact with TCF in the bound states and the transition state is shown in Fig. S7. The majority of contacts are concentrated within the residue range 340-500, which corresponds to the A2 subregion responsible for stabilizing the complex. Notably, there are no contacts established in the terminal subregions A1 and A3 during the transition state, suggesting a folding-assisted unbinding mechanism originating from the A2 subregion of β-catenin.

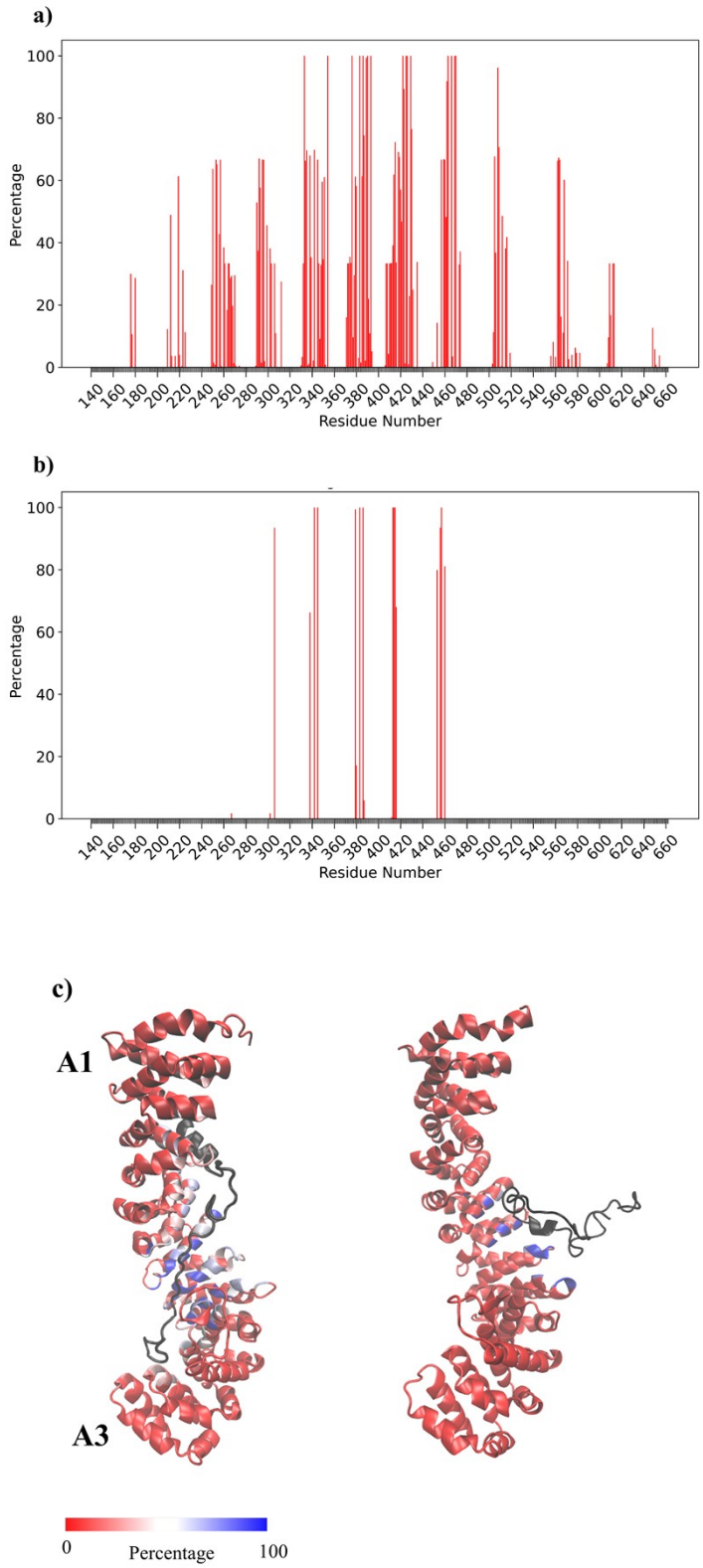

Figure S7. Fraction of key contacts formed between the TCF and residues of β-catenin (residue numbers 140-663) within a cut-off distance of 0.5 nm in the a) bound states (B1, B2 and B3) together b) transition state c) structural representation of the fraction of contacts in all the bound states (left) and transition state (right).

VI. Variation of secondary structural parameters in TCF

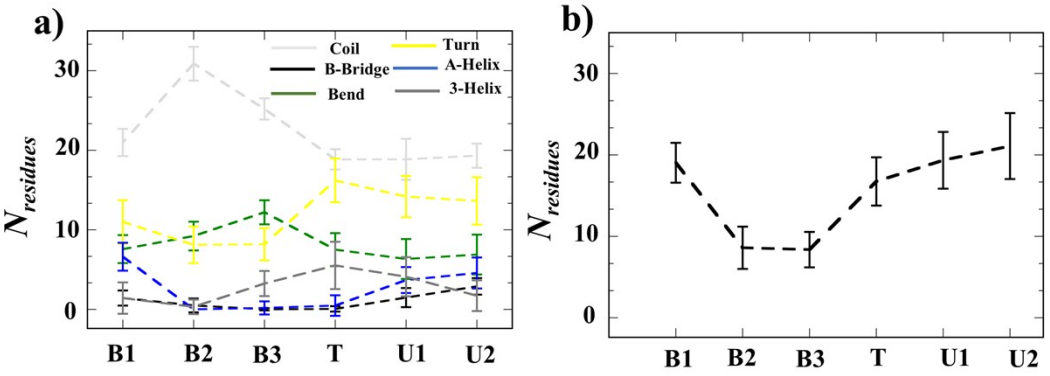

Figure S8. a) Variation of the number of residues involved in the formation of various structural elements (Coil, B-Bridge, Bend, Turn, A-Helix, 3-Helix) in TCF during the unbinding pathway b) Fraction of secondary structure content (helix+bridge+turn) in the states B1, B2, B3, T, U1, and U2.

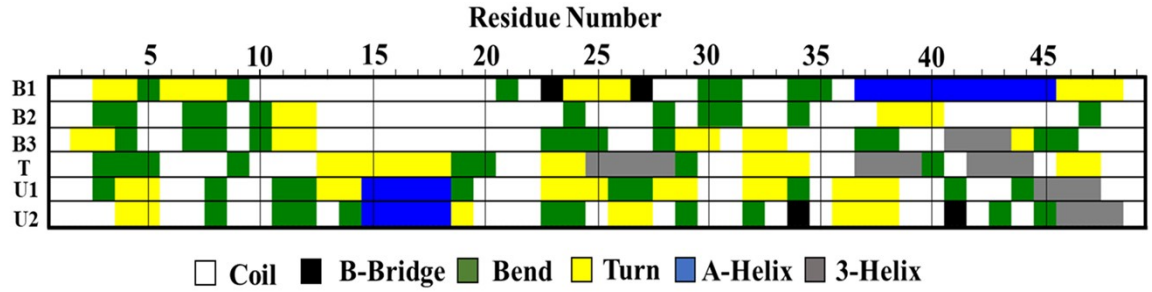

Figure S9. Residue-wise variation of secondary structural content in TCF in the states B1, B2, B3, T, U1, and U2. Structural elements are shown in the inset.

VII. Variation of secondary structural parameters in β-catenin

Variation of the number of residues involved in the formation of different secondary structural elements in β-catenin provided in Fig. S10. As shown in Fig. S10, A-helix is found to be a major secondary structural element (>300 residues) present in the β-catenin followed by turn, coil, and bend structural factors(<300 residues and > 25 residues). All the other secondary structural elements (3-Helix, B-Sheet, 5-Helix, B-Bridge) were found to be in less fraction in the structure of β-catenin (<25 residues). The secondary structural content of β-catenin in specific regions A1, A2, and A3 is shown in Fig. S11. The secondary structural elements in the terminal regions A1 and A3 are found to be unaltered during the unbinding pathway. As shown in the Fig. S11b, it is observed that

the A-helix content was reduced in the A2 sub-region β-catenin, where the final detachment of TCF from the transition state has occurred (Fig. 6).

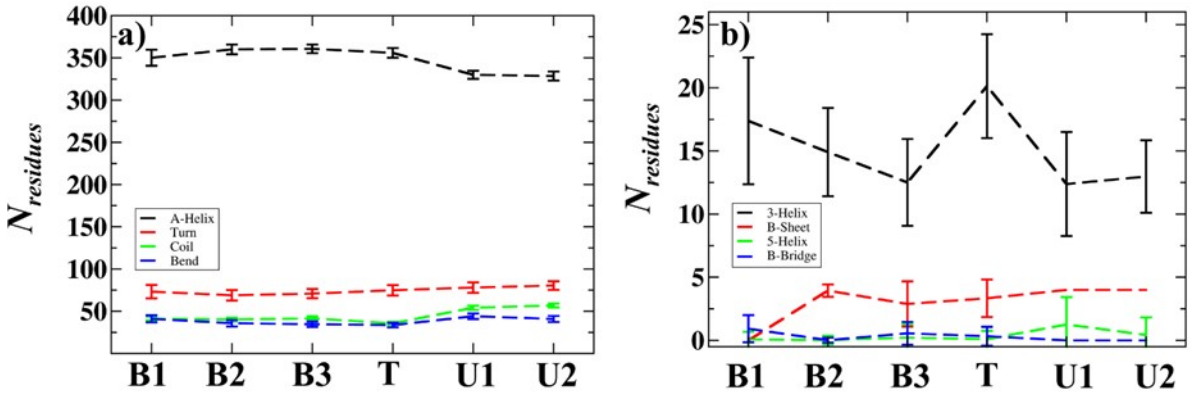

Figure S10. Variation of the number of residues involved in the formation of different secondary structural elements in β-catenin a) A-Helix, Turn, Coil, Bend b) 3 -Helix, B-sheet, 5-Helix, B-Bridge).

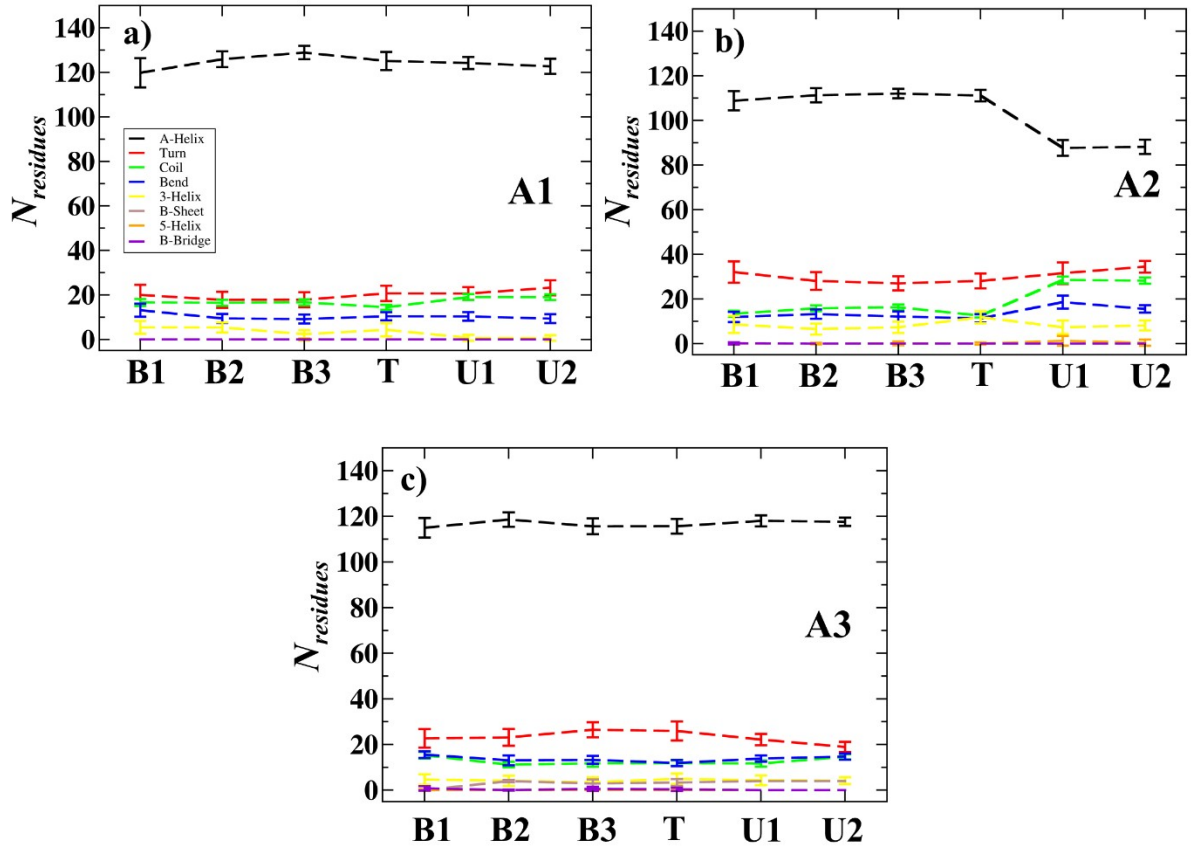

Figure S11. Variation of the number of residues involved in the formation of different secondary structural elements (A-Helix, Turn, Coil, Bend, 3-Helix, B-sheet, 5-Helix, B-Bridge) in specefic regions β-catenin during the unbinding pathway. a) A1-region b) A2-region c) A3-region. A decrease in the A-helix content is observed in the unbound states of the A2 region.

VIII. Variation of the radius of gyration and root mean square deviation (RMSD) in the heavy atoms of β-catenin and TCF

The variation of radius of gyration and RMSD in the heavy atoms of β-catenin is shown in the Fig. S12 and Fig. S13 respectively. As shown in Fig. S12, the radius of gyration of heavy atoms of β-catenin maintains a value between 3.3 nm and 3.7 nm throughout the dissociation process. However, the radius of gyration of heavy atoms of the TCF decreased steadily from bound states to unbound state U1, resulting in folded states of TCF, as discussed in the main manuscript. A higher RMSD is observed in TCF compared to β-catenin due to the transition from elongated structure to compact folded structure in TCF. Relatively higher RMSD (>0.6 nm) is observed in the unbound state of β-catenin compared to bound states due to the reduction of A-helix content in the A2 subregion (as shown in Fig. S11b).

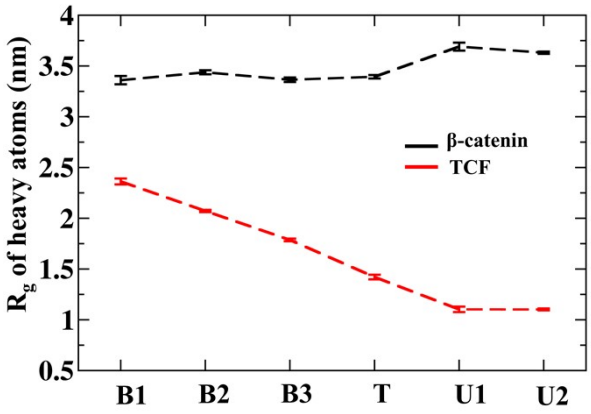

Figure S12. Variation of radius of gyration in the heavy atoms of β-catenin and TCF during the unbinding pathway.

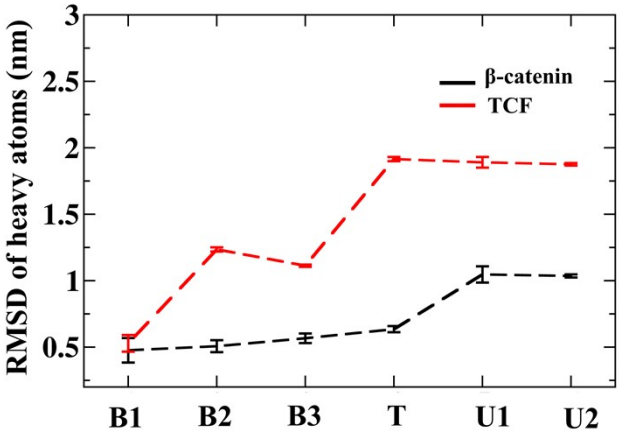

Figure S13. Vriation of RMSD in the heavy atoms of β-catenin and TCF with respect to the equilibrated complex structure during the unbinding pathway.

IX. Variation of hydrogen bonds during the unbinding pathway

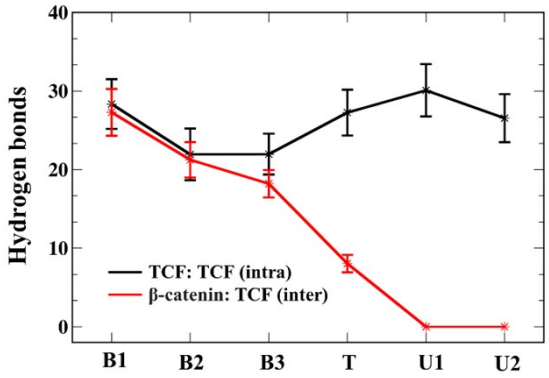

Figure S14. Variation of Intramolecular hydrogen bonds in TCF (black) and Intermolecular hydrogen bonds (red) between β-catenin and TCF during the unbinding pathway.

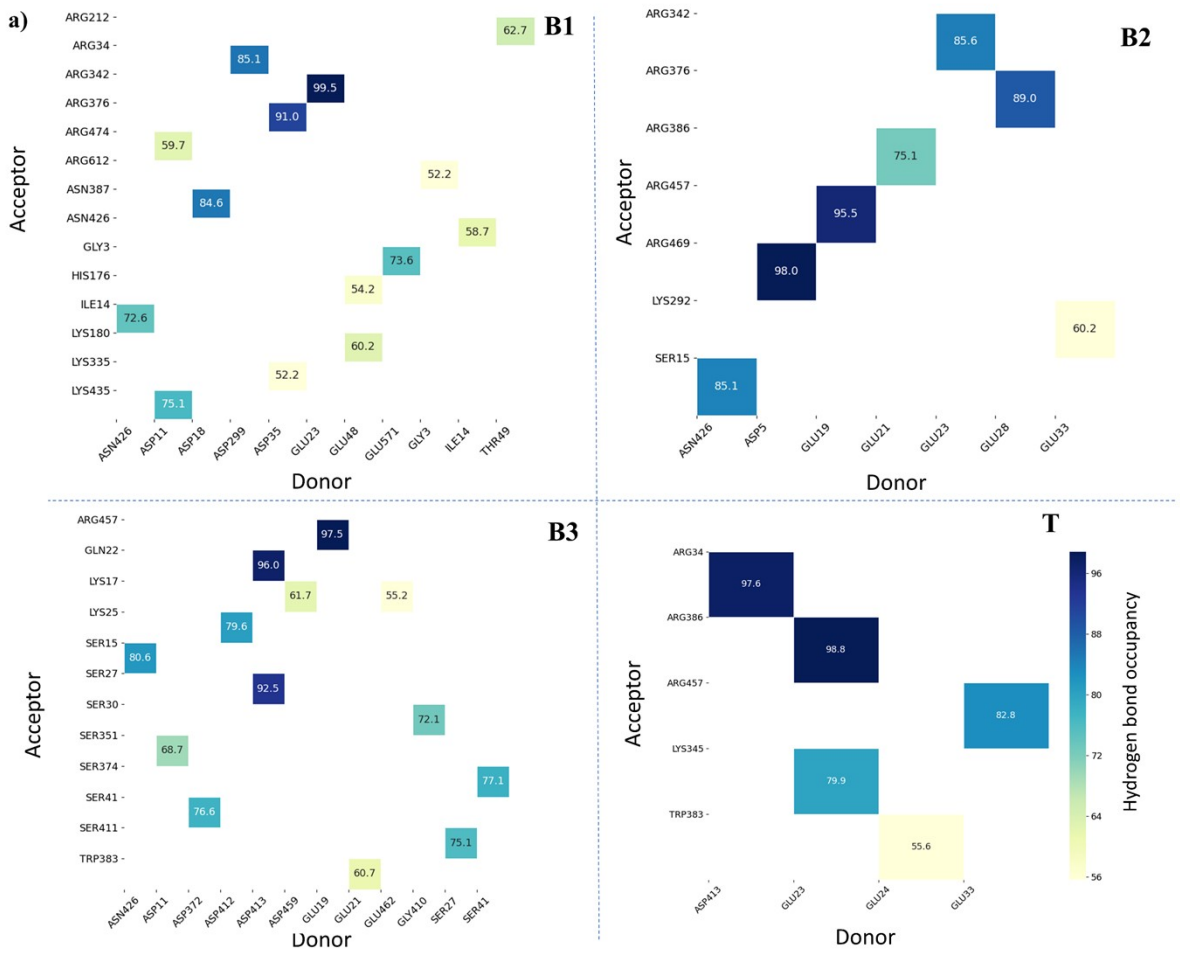

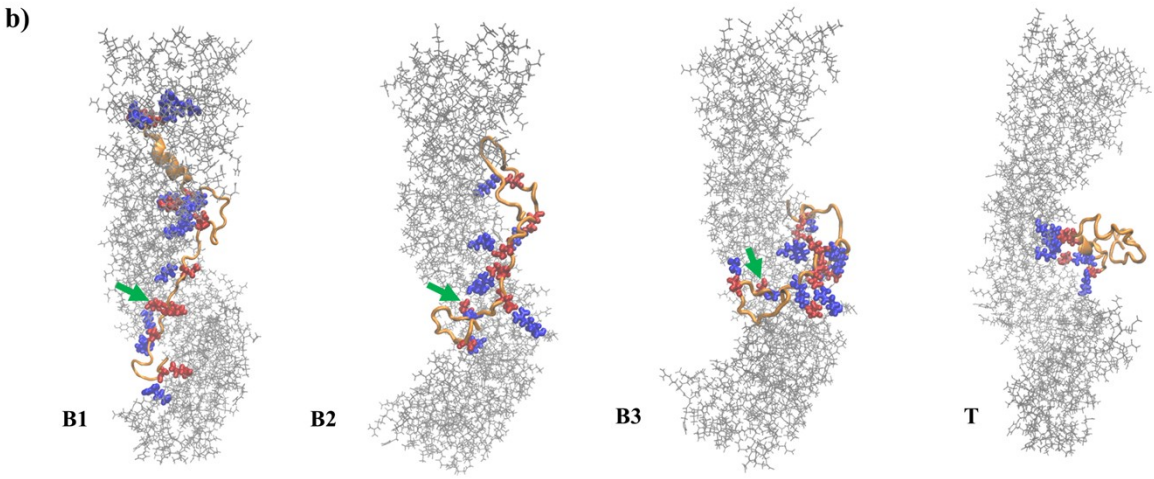

Figure S15. a) Intermolecular hydrogen bond occupancy maps in percentage (between donor and acceptor residues in β-catenin: TCF complex) for interactions persistent through at least 50% of the structures present in the bound states (B1, B2, B3) and transition state (T). b) Representation of donor (highlighted in red) and acceptor residues (highlighted in blue) in the bound states and transition state of β-catenin:TCF complex according to hydrogen bond occupancy map. β-catenin and TCF are shown in grey and orange, respectively. ASN426 residue in β-catenin consistently serves as a hydrogen bond donor across all these states. ASN426 residue (highlighted by green arrow) in β-catenin consistently serves as a hydrogen bond donor across all the bound states.

X. Role of the hotspot residues in the dissociation/folding of TCF

Monitoring the variation of root mean square deviation (RMSD) of hotspot residues in the β-catenin with respect to the equilibrated structure during the unbinding pathway suggests that hotspot 5 plays an important role in the unbinding of TCF. Fig. S16 shows the variation of RMSD within the various hotspots of β-catenin. The higher RMSD values (> 0.4 nm) in the hotspot 5 in the unbound states (U1 and U2) suggest that there were significant changes in hotspot 5 of β-catenin after the detachment of TCF. This suggests that hotspot 5 could be an interesting region for further drug discovery studies.

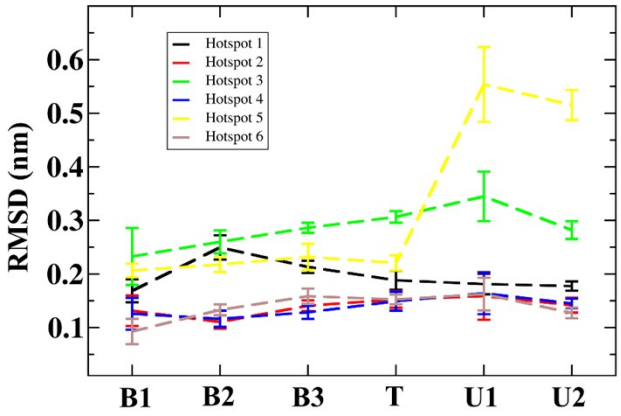

Figure S16. Variation of RMSD in the hotspot residues of β-catenin during the unbinding pathway.